Sonderdruck aus:

COSPAR

SPACE RESEARCH XIII

Proceedings of Open Meetings of Working Groups
on Physical Sciences of the Fifteenth Plenary Meeting of COSPAR

MADRID, SPAIN, 10—24 May, 1972

Organized by

THE COMMITTEE ON SPACE RESEARCH—COSPAR

and

THE 'COMISION NACIONAL DE INVESTIGACION
DEL ESPACIO'' OF SPAIN

Edited by

M. J. RYCROFT
S. K. RUNCORN

AKADEMIE-VERLAG · BERLIN
1973

Space Research XIII — Akademie-Verlag, Berlin 1973

THE ALADDIN EXPERIMENT — PART II, COMPOSITION

C. R. PHILBRICK[a], R. S. NARCISI[a], R. E. GOOD[a], H. S. HOFFMAN[a], T. J. KENESHEA[a], M. A. MACLEOD[a], S. P. ZIMMERMAN[a] and B. W. REINISCH[b]

[a]Air Force Cambridge Research Laboratories, Bedford, Mass., USA
[b]Lowell Technological Institute Research Foundation, Lowell, Mass., USA

Vertical profiles of N_2, O_2, Ar, O, CO_2, O_3, $O_2(^1\Delta_g)$, total neutral density and temperature were measured in the ALADDIN experiment. The measured turbulent and molecular diffusion coefficients, total mass density and temperature were used as inputs to model the profiles of O, O_2, and other neutral constituents which are compared with the corresponding measurements. Emission of $O_2(^1\Delta_g)$ showed a peak density at 82 km of 1.3×10^9 cm^{-3}, corresponding to an ozone density peak of 6×10^7 cm^{-3}. Oxidation of lithium released as a tracer decreased rapidly from 85 to 100 km, requiring a Li—Li—M reaction to account for the observations. A blanketing Es layer was observed to increase from 3.5 MHz at launch to 8 MHz two hours later, possibly associated with Al^+ ions formed during the chemical releases used for wind and temperature profiles. Positive ion composition measurements showed a meteoric ion layer at 108 km composed mainly of Si^+ with Mg^+, Na^+, Fe^+, Ca^+, Ni^+, and SiO^+ which corresponds to a 3.5 MHz blanketing sporadic-E layer seen with a ground-based ionosonde. Al^+ associated with the chemical release of $Al(CH_3)_3$ was measured in two regions of the flight; calculations of the effect of wind fields on the ion density distributions show ion density profiles which generally agree with the measurements.

1. Introduction

The atmospheric dynamics measurements of the ALADDIN 1 program have been presented by Rosenberg et al. [1]. Here a brief summary of the electron and ion density and ion composition measurements are presented and compared with a theory for the E region [2—4]. An explanation of the inventory of lithium after its release as a vapor in the 80—100 km region is given [5]. Photometer measurements of $O_2(^1\Delta_g)$ have been used to infer O_3 and O densities [6]. The neutral atmospheric composition measured with a mass spectrometer has been compared with an atmospheric model which determines the vertical time dependent profiles of the constituents using the measured parameters relating to the dynamical processes [7, 8].

2. Ion Composition and Electron Density

Close to the launch site at Eglin AFB a Digisonde 128 was monitoring the ionosphere. E-region ionograms were recorded with 1.5 km height range sampling and 25 kHz frequency increments. These ionograms indicated a moderate activity of sporadic E during the month of November, sometimes with up to three layers occurring simultaneously. In the ten days surrounding the launch day, i.e. from 13 to 22 November 1970, the *f*oEs values always remained below 4 MHz. On 20 Nov-

ember, foEs reached a peak of 5.8 MHz and decreased to 3.5 MHz before the launch. Two hours after the chemical release foEs reached 8 MHz and this high electron density is probably associated with the released chemicals. The high Es activity carries on into the next day and then levels off.

The strong Es occurrence during the launch time made the detection of the normal E-region ionization very difficult. The resulting E-region electron density profiles, therefore, contain large error bars, see Fig. 1. Sporadic E layers were located at 100 km and 108 km before the launch. These layers moved down by one kilometer during the launch program and another layer appeared at 102 km.

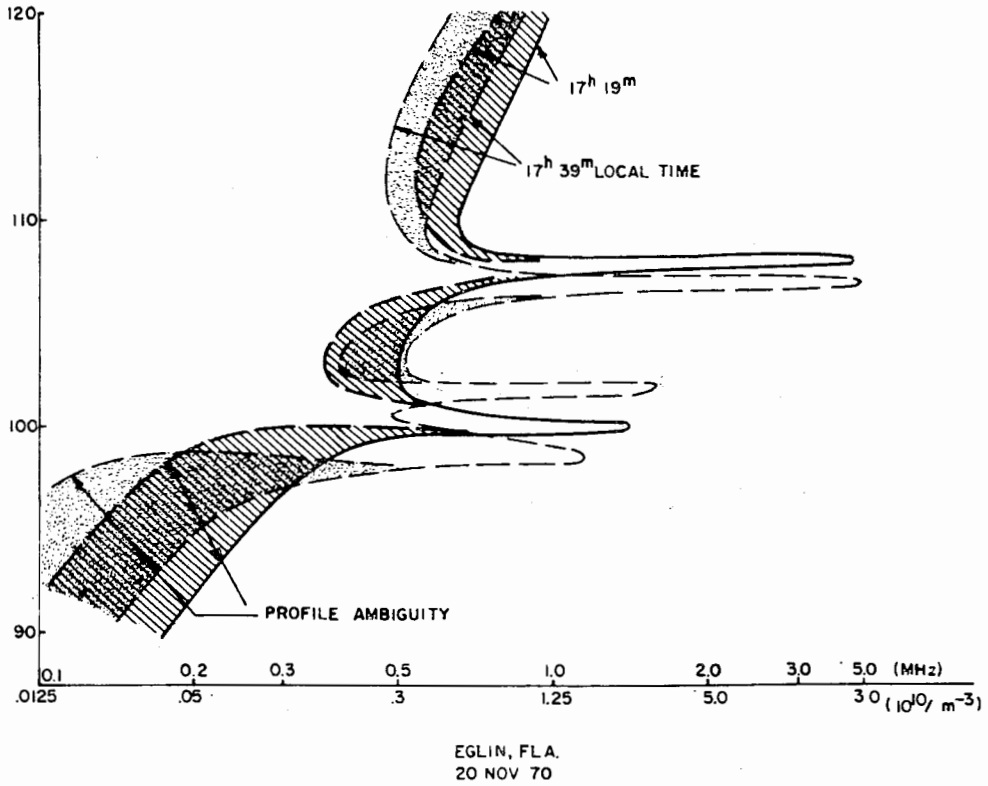

Fig. 1. E-region electron profiles near the time of launch.

A positive ion mass spectrometer was used to obtain composition measurements shown in Fig. 2. The major positive ion species concentrations are shown as a function of altitude between 85 and 140 km on vehicle ascent. The main features are the omnipresent metallic ion layer consisting mainly of iron and magnesium together with other meteoric species in the vicinity of 95 km, extending from 88 to 102 km. Above the metal ion layer near 98 km, nitric oxide and molecular oxygen ions become dominant. At 108 km, a thin meteoric ion layer was observed both on upleg and downleg. This layer was composed of mainly Si^+ with Mg^+, Fe^+, Na^+, Ca^+, Ni^+, and SiO^+. Where the meteoric ions were dominant, NO^+ was greatly reduced. The altitude resolution of the mass spectrometer is limited by the 1.5 seconds required for a mass spectrum scan, and thus the peak density of the meteoric ions in this layer may not be well defined by the spectrometer measurement. The digisonde showed peak density for a thin layer at this altitude, indicated by the "X" in Fig. 2. At higher altitudes, two layers of Al^+ were observed. The

lower one, centered around 122 km and extending from 114 km to 128 km, can be attributed to Al^+ ions formed after the release of TMA, $Al(CH_3)_3$, from a chemical wind trail rocket launched four minutes before the mass spectrometer payload. The motion of the Al^+ ions formed in the vicinity of the chemical release has been calculated using the sporadic E theory of MacLeod [9]. Although the detailed chemistry resulting in the formation of the Al^+ is not understood, the Al^+ layers have been observed previously when measurements were made with chemical releases [10]. The distribution of the low altitude Al^+ ion profile shows reasonable agreement with the Al^+ ion trail position calculated by utilizing the TMA trail

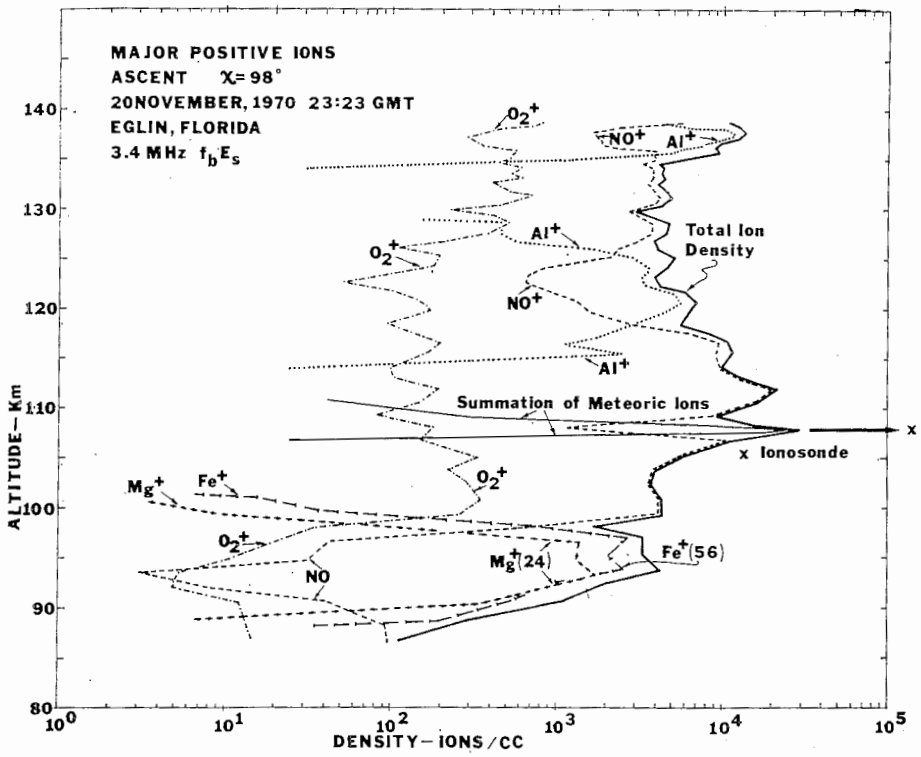

Fig. 2. Mass-spectrometer measurements of positive ion composition.

position and the ion motion deduced from ion—neutral collision forces and geomagnetic Lorentz forces. The higher altitude Al^+ layer near 138 km probably resulted from the TMA release also; however, the above forces do not provide sufficient motion of the Al^+ to move the ions into the flight path of the mass spectrometer. If some additional force were acting on the ion distribution, it would have to be significant. For instance, if an electric field was assumed as a driving force a field strength of about 10 mV m^{-1} would be required. In the region where these two Al^+ ion layers occur, a significant depletion of the NO^+ is also observed which occurs because of recombinative loss of NO^+ with electrons and perhaps charge transfer to metal atoms as well. At altitudes where the atomic—ion species are either absent or present in relatively small concentrations, NO^+ is the dominant species with O_2^+ varying from 1% to 10% of the NO^+ concentration.

3. E-Region Model

Theoretical ion density profiles were computed by integrating the time-dependent coupled continuity equations for an ionospheric model containing the species NO^+, O_2^+, N^+, O^+, M^+ and e. The calculation builds up the background ionization (except the metal M^+) from solar photoproduction beginning at noon on the experiment day. As the model time advances into the evening, the photoproduction is reduced, and the chemistry is dominated by the charge exchange and dissociative recombination reactions. At a preset time (here taken to be 2000 sec before the positive ion mass spectrometer flight time) the effect of the ion winds is introduced

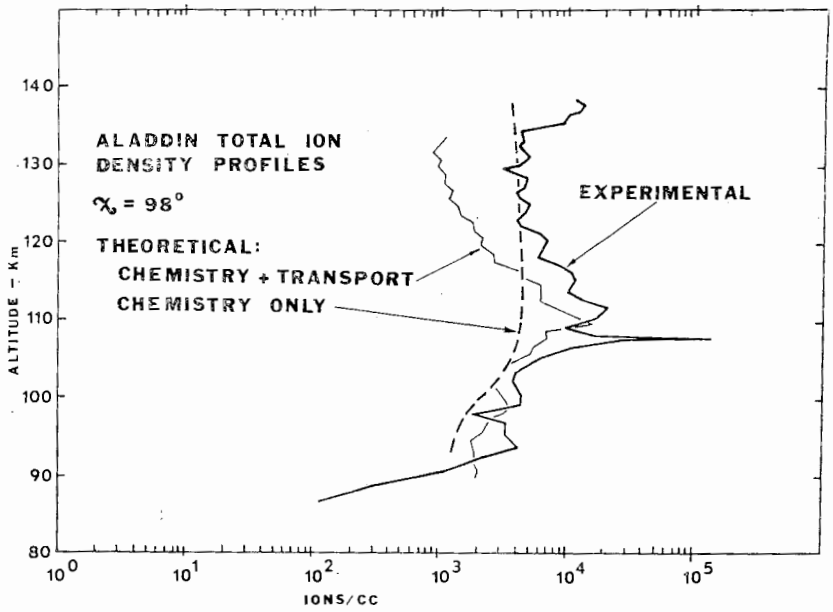

Fig. 3. Comparison of theoretical and measured positive ion density.

by adding the divergence of the ion flux to the continuity equations (using ion winds calculated from the measured neutral winds). Simultaneously metal ions with a density of 1000 cm^{-3} are added throughout the range 90—137 km. The integration is then carried on until the experiment time (2323 GMT, $\chi = 98°$). The total ion density profile obtained in this manner is shown in Fig. 3, together with the experimental profile and a profile calculated leaving out the ion transport contribution. Although the effect of ion transport is clearly seen and results in a better prediction than the chemistry only profile, the agreement between theory and experiment is poorer than was obtained previously [11]. The peak at 110 km is due to the layering of the metal ions at the zero of the vertical ion velocity profile, and is 2 km higher than the experimental peak. The (chemistry + transport) curve does not reproduce well the small-scale variations of the experimental profile. Both discrepancies may reflect the influence of short period motions which cannot be taken into account by the model at the present time. Although the sources of the differences between the measured and calculated curves may be sought among a variety of effects which are not presently included in the calculations, some improvement will undoubtedly result when refinements of the present model are introduced.

4. Lithium Chemistry in the Upper Atmosphere

Lithium vapor was released at altitudes of 80—100 km. The measurements of the 6708 Å Li atom emission spectrum were analyzed to determine the lithium inventory as a function of altitude and time after release. It was found that lithium is consumed extremely rapidly at the lower altitudes. At 85 km, only 1% of the lithium released was observed after 3 seconds, while at 100 km, 40 % of the released lithium was observed after 3 seconds. At these altitudes simple oxidation reactions of monatomic lithium by atomic and molecular oxygen or by ozone cannot account for such rapid disappearance of the vaporized lithium. It is necessary to include reactions involving dimerized lithium or termolecular reactions in which two lithium atoms participate. High density conditions exist during the initial expansion at lower altitudes which enhance such reactions significantly. The simple oxidation reactions become the dominant mechanism of lithium consumption a minute or so after release.

5. Twilight $O_2(^1\Delta_g)$ Measurements

The volume emission rate profile of the measured $O_2(^1\Delta_g)$ is shown in Fig. 4. The instrumentation consisted of a 120 Å width IR filter centered at 1.279 μ. The signal was detected with a PbS detector with a 0.1 second time constant using synchronous detection. A peak in the emission rate profile was observed near 83 km.

The $O_2(^1\Delta_g)$ observations in the mesosphere can be used to calculate the densities of atomic oxygen and ozone under the assumption of steady-state photo-

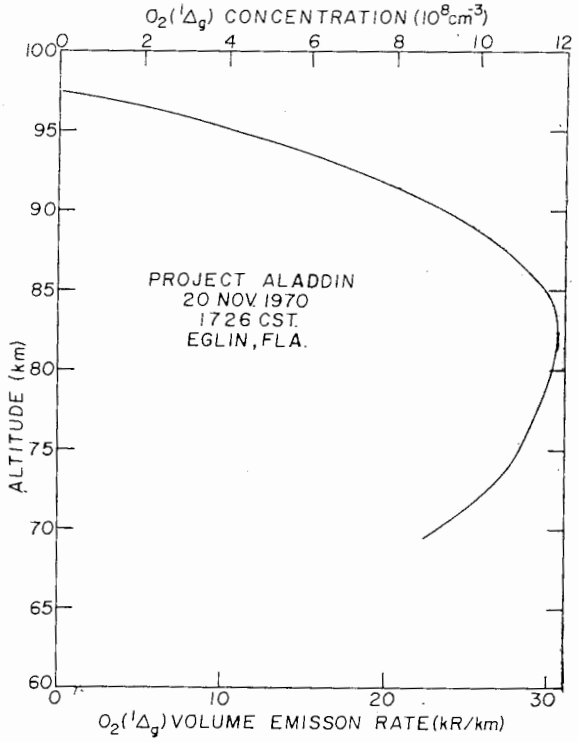

Fig. 4. Measured volume emission rate profile of $O_2(^1\Delta_g)$.

chemical equilibrium. It can be shown that the rate of loss of ozone by hydrogen is only 4% of the daytime dissociation rate and can be neglected. Another factor which is important to the computation of atomic oxygen density during twilight is that the relationship is independent of the solar dissociation rate. Using the mass-spectrometer measurements of N_2 and O_2 and the photometer measurements of $O_2(^1\Delta_g)$, together with the measured temperature and density, the following species concentrations were calculated.

Altitude (km)	$O_2(^1\Delta_g)/cm^3$	O/cm^3	O_3/cm^3
85	1.2×10^9	7.2×10^{11}	4.5×10^7
90	8×10^8	1.1×10^{11}	2.8×10^7

6. Neutral Composition

Measurements of the neutral composition, shown in Fig. 5, were obtained with a cryosorption pumped RF quadrupole mass spectrometer [12, 13]. Two ionization energies were used to extend the range of the atomic oxygen measurement to lower altitudes. The lower altitude points on the O profile may be in error because of the large signal from dissociative ionization of O_2 which was removed from them. At the 90 km level, the ground level mixing concentrations are shown in Fig. 5 and the measurements are in good agreement. Comparison of the Ar and N_2 densities shows a mixed atmosphere to an altitude about 105 km. The variations shown in the O profile generally reproduce on ascent and descent. The atomic oxygen density should be viewed as a lower limit for the present time. Tests are planned over the next several months which should help establish the accuracy. The total density profile was obtained from the measured mass density of Theon

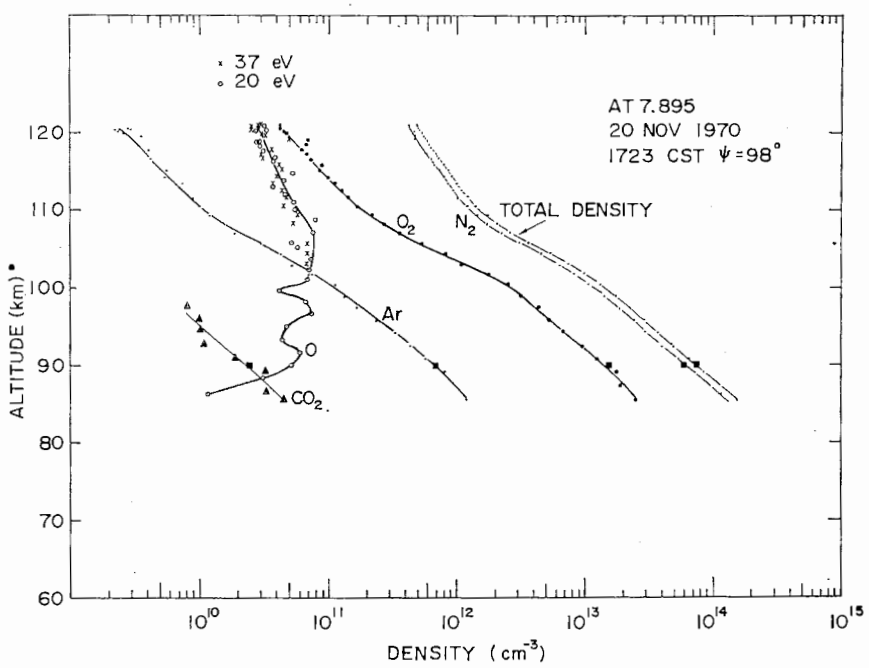

Fig. 5. Mass spectrometer measurements of the neutral atmospheric composition.

and Horvath [14] and the mean molecular mass measured by the mass spectrometer.

A theoretical computer calculation of the distribution of the species O, O_2, and Ar follows directly from the procedure given by George et al. [15]. The major difference is that here the mass density, temperature, and both the turbulent and molecular diffusion coefficients were determined directly from measurements during the ALADDIN 1 program. The calculation was performed for 30° N latitude with a solar declination angle of −15° and the O and O_2 densities at the upper boundary of 150 km are those determined by flux continuity.

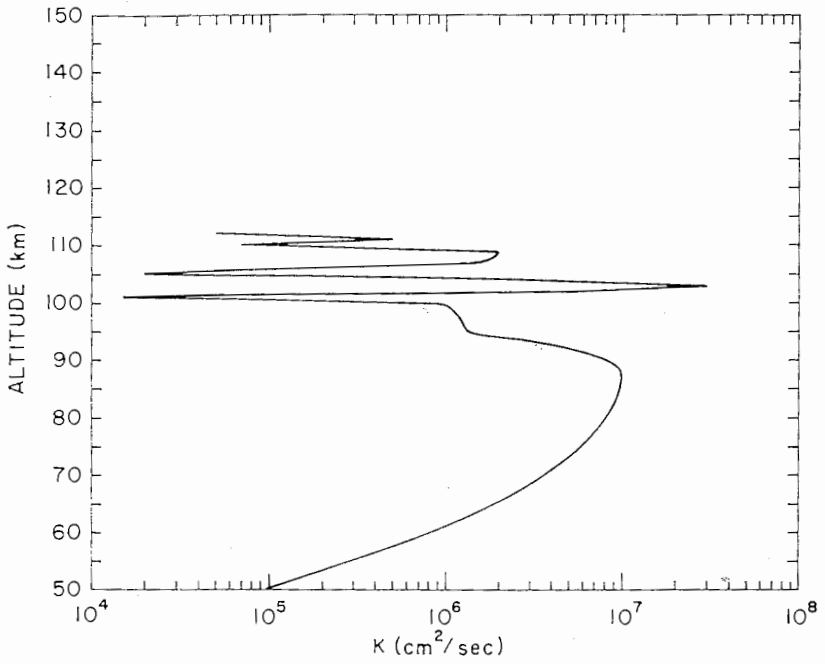

Fig. 6. Measured turbulent diffusion coefficients from the chemical releases.

The determination of the vertical turbulent diffusion coefficients is based upon measurements of the rate of dissipation of turbulent kinetic energy and the measured temperature of Theon and Horvath [14], and yields only a lower limit. The results of these diffusion calculations are shown in Fig. 6, where the turbulent layers are separated by laminar regions. The diffusivity in the altitude region below 93 km, where turbulence could not be measured, was estimated to fit Johnson and Wilkins [16] calculations of turbulent heat transfer.

The calculated profiles of the minor species are shown in Fig. 7. Two values of the vertical turbulent diffusivity were used, the lower limiting value K and an arbitrary factor of three times this value, $3K$. The agreement between the mass-spectrometer measurements and the calculated profile is fairly good, with the exception of the argon distribution above 105 km and the atomic oxygen distribution below 90 km. The discrepancy in the argon profile can be rectified if the turbulent diffusivity in the layer at 110 km was amplified over the other layers. This change may also improve, still further, the calculated O distribution. Also, the calculated O profile below 90 km may be in error due to our lack of measurements of turbulence in this region and the assumptions about the turbulent

diffusivity there. It is interesting to note that the dips in the measured profile near 93 and 100 km are also indicated in the calculated profile.

Although the analysis and comparison of these measurements is not yet complete, the importance of comparing the dyamical processes with the distribution of ion and neutral species is apparent. This experiment has been followed by the recent ALADDIN 2 program (April 1972) and will be continued and expanded in the ALADDIN 3 program in late 1973.

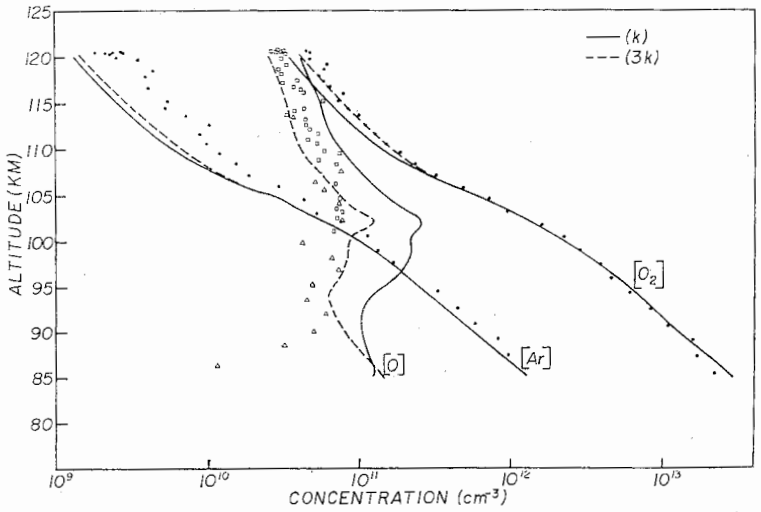

Fig. 7. Comparison of the theoretically computed neutral composition for the conditioning of the 20 November experiment with the measured points.

References

[1] N. W. ROSENBERG, D. GOLOMB, S. P. ZIMMERMAN, W. K. VICKERY and J. S. THEON, Space Research XIII, 435 (1973).
[2] B. W. REINISCH and K. BIBL, Trans. Am. Geophys. Un. **53**, 462 (1972).
[3] R. S. NARCISI, C. R. PHILBRICK, M. A. MACLEOD and N. W. ROSENBERG, Trans. Am. Geophys. Un. **53**, 462 (1972).
[4] M. A. MACLEOD, T. J. KENESHEA and R. S. NARCISI, Trans. Am. Geophys. Un. **53**, 464 (1972).
[5] H. S. HOFFMAN, Trans Am. Geophys. Un. **53**, 463 (1972).
[6] R. E. GOOD, Trans Am. Geophys. Un. **53**, 463 (1972).
[7] C. R. PHILBRICK and G. A. FAUCHER, Trans. Am. Geophys. Un. **53**, 463 (1972).
[8] T. J. KENESHEA, J. D. GEORGE and S. P. ZIMMERMAN, Trans. Am. Geophys. Un. **53**, 464 (1972).
[9] M. A. MACLEOD, J. Atmos. Sci. **23**, 96 (1966).
[10] R. S. NARCISI, D. M. THOMAS, A. D. BAILEY and L. DELLA LUCCA, Trans. Am. Geophys. Un. **50**, 654 (1969).
[11] T. J. KENESHEA and M. A. MACLEOD, J. Atmos. Sci. **27**, 981 (1970).
[12] C. R. PHILBRICK, G. A. FAUCHER and R. A. WLODYKA, AFCRL Rep. No. 71-0602 (1971).
[13] C. R. PHILBRICK, G. A. FAUCHER and E. TRZCINSKI, Space Research XIII, 255 (1973).
[14] J. S. THEON and J. J. HORVATH, Trans. Am. Geophys. Un. **53**, 463 (1972).
[15] J. D. GEORGE, S. P. ZIMMERMAN and T. J. KENESHEA, Space Research XII, 695 (1972).
[16] F. S. JOHNSON and E. M. WILKINS, J. Geophys. Res. **70**, 1281 (1965).